Research Article

Naveen Prakash Noronha* and Krishna Munishamaih

Performance assessment of a balloon assisted micro airborne wind turbine system

https://doi.org/10.1515/ehs-2021-0018
Received August 12, 2021; accepted October 9, 2021;
published online October 22, 2021

Abstract: This study intends to examine the performance of a balloon-assisted micro airborne wind turbine in a low wind speed location. The influence of the balloon separation gap on the airborne wind energy system (AWES) performance is also explored. A micro-AWES with a diameter of 3 m and a power output of 1 kW was fabricated and tested at 50, 100, 150, 200, and 250 m. Further, the optimum separation spacing of 13 m was maintained between the balloon and the ducted turbine to reduce balloon turbulence on the turbine. The airborne wind turbine achieved a maximum power output of 250 W at 250 m height while the average wind speed remained 6 m/s. The maximum power coefficient obtained was 0.25 while annual energy production (AEP) remained 1200 kWh. The low power coefficient is credited to the turbulence and drifting in the airborne system and the drag caused by the airborne structure. While a cost-effective commercial model of micro AWES is still being developed, the present work attempts to harvest wind energy at high elevations in low wind speed areas.

Keywords: airborne systems; high altitude wind energy; jet streams; microturbine; wind turbine.

Introduction

The standard land-based wind turbine technology has matured and been scaled up to the full capability to harness wind resources in many locations of the world. The energy industry explores novel ways to harness wind energy without experiencing land or wind challenges due to low wind speeds and a lack of sufficient space for ultra-mega wind farms. The solution to these issues is decentralised small aerial wind turbines that can be deployed practically any place. The high-altitude flying wind turbine concept dates back to 1943 when a patent was submitted in the USA for an innovative design for harvesting wind energy at a higher altitude.

During WWII, the ground-breaking technology of a wind-powered system was built intended to be employed in emergency scenarios to transport a bomber. Its applications were later expanded to include energy production at higher heights. Furthermore, when fuel prices rose, so did interest in airborne energy, leading to submitting an identical concept to the United States patent and trademark office in 1976. However, as oil prices collapsed in the early 1980s, interests in airborne wind technology development faded, and until recently, relatively few patents were registered. Growing public awareness of the benefits of renewable energy and greater investment in land-based wind power production systems has led to the growing research interest in airborne wind generation. The immensity of the source, the requirement for limited land space, and the low cost per unit of electricity are three significant elements contributing to the growing interest in airborne wind energy technology.

Commercial and scientific groups have proposed a range of ways for capturing wind energy at high altitudes, including high altitude rotating systems, tethered fixed winglet vehicles, kites, and rotorcrafts (Argatov, Rautakorpi, and Silvennoinen 2009; Baheri and Vermillion 2017).

Manalis (1976) described a work in which aerial systems were employed to deploy the aerogenerator on communication aerostats. These high-altitude aerostats were utilised as platforms for vast area communication and broadcast purposes. The investigations were focused on the viability of utilizing aerial wind energy generating systems without increasing the payload of the communication systems and the angular position of the system.

Fagiano, Milanese, and Piga (2010) invented kite energy technology, a unique airborne wind energy device

***Corresponding author: Naveen Prakash Noronha,** Department of Mechanical Engineering, R. V. College of Engineering, Bangalore, India, E-mail: nannupn@gmail.com. https://orcid.org/0000-0002-7835-8630
Krishna Munishamaih, Department of Mechanical Engineering, R. V. College of Engineering, Bangalore, India,
E-mail: krishnam@rvce.edu.in

to harness power at higher altitudes. In this work, the researchers focused on three key objectives: first, assessing the used control mechanism, second, optimising the generator performance, third, continuous power generation delivering constant and maximum power.

Hwang, Kang, and Kim (2011) introduced a cycloidal wind turbine utilising a cycloidal blade to harvest the wind energy at higher elevations. The entire system was put on the tethered balloon, and the power supplied by the turbine was modified using modifying the pitch of the rotor. In their experiment, the researchers claimed to produce 30 kW power at 500 m height, which is three times the power at the ground level.

Boyerahmadi, Amjady, and Rezaey (2012) developed an approach of classification which classifies the hitherto study on airborne wind turbine technology. In their work, researchers categorically classified the airborne power production systems based on the mechanism employed, the airborne method used, and the capacity of the airborne generator system. The researchers reviewed a thorough list of airborne technologies to provide a clear notion to the other researchers for the comparison investigation.

Zanon et al. (2013) sought to produce electrical energy by a tethered airfoil unfolded at higher altitudes with high velocity. The researchers noted the increase in drag owing to the single airfoil creating a detrimental impact on the entire efficiency of the system. The researchers constructed a pair of airfoils attached to the single tether to overcome this issue, which resulted in reduced drag. The researchers also observed that a higher efficiency level might be attained by correctly balancing the airfoil trajectories. Based on these pair of airfoils performance, the researchers suggested a mathematical approach to model the multi-airfoil based airborne energy generation system. However, studies concluded that dual-airfoil designs are less efficient at a big scale.

The literature review described above and many more papers have examined the design of several airborne wind turbine systems. However, the evaluation of the performance of airborne wind turbines at varied balloon separation intervals is not yet conducted. While substantial progress has been achieved in capturing wind energy at high altitudes, the balloon-borne micro aerial energy extraction system is still in its early phases. This project intends to examine the performance of a micro airborne wind turbine system at moderate altitudes. The present research work is separated into two phases: firstly, design of the airborne system, secondly, testing of the airborne system at various heights considering the optimum separation distance. The BEM based wind turbine design approach given in reference (Manwell, McGowan, and Rogers 2010) is employed in the present work. The entire design process begins with identifying the chord length, twist, pitch, airfoil configuration, balloon size, and necessary helium volume for a safe lift. The performance evaluations were carried out on the R. V. College of Engineering campus, Bangalore, India, which is 3000 feet above sea level.

Design methodology of the airborne wind energy system

Wind power analysis

Wind turbines are unique machines that convert the kinetic energy inherent in the air into mechanical energy. However, various aspects influence the conversion process, including wind speed (v) m/s, air density (ρ) kg/m^3, and rotor swept area (A) m^2. Because the kinetic energy of air is proportional to its mass per unit volume or density, denser air has higher kinetic energy. Furthermore, the kinetic energy in the wind is related to the square of the wind velocity, making high-speed winds more favourable than low-speed, denser winds (Rajab et al. 2019). So, the kinetic energy present in the wind can be expressed by the general kinetic energy relation expressed in Eq. (1).

$$E_k = 1/2mv^2 = 1/2\rho Vv^2 = 1/2\rho Adv^2 \quad (1)$$

In the above expression, m is the mass of the wind in kg, v is the wind speed at sea level in m/s, ρ is the density of the air in kg/m^3, A is the swept area of the turbine rotor in m^2, and d is the thickness or depth of the imaginary air disc in m.

The rate of energy consumption is viewed as the power of the system. In the present example, E_k generated per second is regarded as the power produced from the wind. Equation (2) relates to the power contained in the wind of area A and velocity v. From Eq. (2), it is evident that the power in the wind is proportional to the cube of the wind velocity.

$$P_{in} = E_{k/t} = 1/2t\ (\rho Adv^2) = 1/2\rho Av^3 \quad (2)$$

Since the power produced by the wind predominantly depends on the wind velocity, the high-velocity wind is the prime requirement for the generation of uninterrupted power.

The wind turbine converts the power present in the wind into mechanical power, as shown in Eq. (3).

$$P_{mech} = \omega T \tag{3}$$

In Eq. (3), ω is the angular speed of the rotor in (rad/s), and T is the wind turbine torque in (Nm).

As per the second law of thermodynamics, one form of energy can not be wholly converted into another form; otherwise, the system becomes a perpetual motion machine. Hence the power present in the wind cannot be wholly converted into usable power, and the maximum limit of conversion is explained by Betz and is famously known as the Betz limit (Bergey 1979). Hence as per Betz limit, the maximum power extractable is 0.593 times the power available in the wind. Therefore the maximum power equation can be re-written as shown in Eq. (4).

$$P_m = 0.5 C_p \rho A v_w^3 \tag{4}$$

where C_p is the coefficient of power and is the ratio of the maximum power developed in the wind turbine to the theoretical maximum power available in the wind for the given swept volume. In Eq. (4), v_w represents the relative wind velocity of the turbine; however, for a turbine with a constant pitch angle, β, the coefficient of power, C_p is the function of tip speed, λ.

If the actual power developed by the turbine is measured as the electrical power produced by the product of voltage, V, and current, I, the turbine's Cp is defined by Eq. (5).

$$Cp = V.I\,(2\rho A v^3) \tag{5}$$

Electrical losses are not taken into account in any of the calculations in this study.

Design of a microturbine

According to IEC 61400.2, there is currently no particular design approach for ducted or diffuser augmented micro airborne wind turbines. The typical design requirement for an open wind turbine with a swept area of less than 200 sq. m is stated in this design code. The working model of the present turbine was made using the injection moulding technique in the small fabrication factory located in Bengaluru, South India. The unique advantage of the injection moulding manufacturing process is its cost-effectiveness while retaining the mass to stiffness ratio. The necessary requirements of a mould, such as a runner, sprue, and ejector pins, were designed using CAD software and then machined using a CNC mill. The moulds were made into two halves to create a blade-shaped mould cavity. The flexible crack-free nylon carbon fiber composite material is used in the making of the blade. A homogeneous mixture needs to be prepared to avoid balancing the blades due to the uneven distribution of carbon fiber composition. The other fixtures, such as bearing mount, duct mount, and turbine mounting arrangements, were prepared in the workshop.

In airborne wind energy systems, a duct is a one-of-a-kind design that fulfils many tasks. When the turbine is positioned in the throat of a nozzle-shaped duct, it improves performance (Dighe et al. 2019a, 2019b); when the duct is cylindrical, it offers a laminar flow across the turbine. This is a separate study in which the turbine performance is enhanced 2.5 times over the initial value, surpassing the Betz limit of 59.3%. The duct used in the present work was not explicitly designed to perform a specific function; instead, it serves as a supporting structure by streamlining the air.

Along with the tail flap, the duct helps keep the turbine always oriented toward the wind, increasing efficiency. As shown in Figure 1, an aluminium rod and a wooden arrangement are used to secure the ducted wind turbine to the duct.

As shown in Figure 2, the concept addressed in this study is based on a balloon-borne airborne system. Tethers keep an aerial system steady and positioned at a specified height and location. The tethers retain the system in place as the wind tries to disrupt it. The airborne assembly comprises a microturbine, duct, balloon, and orienting flap. The CFD design approach has been validated from the wind tunnel data received from reference (Kesby, Bradney, and Clausen 2017) and the design and performance analyses are detailed in the author's earlier publications.

Electrical system design

Small wind turbine manufacturers have found it challenging to develop an efficient electrical system that works in unison with the turbine output. Faulty generator electrical controller design has had a significant impact on small wind turbine design (Wood 2010). Permanent magnet generators (PMGs) are currently utilised in most small-scale wind turbine designs due to recent cost and physical size reductions. In this study, a 1 kW PMG is used to generate electricity from an airborne wind turbine. A detailed study about PMG selection of small wind turbines is referred from (Khalil, Alfaitori, and Asheibi 2016; Zafar, Gadalla, and Al-Naiser 2016).

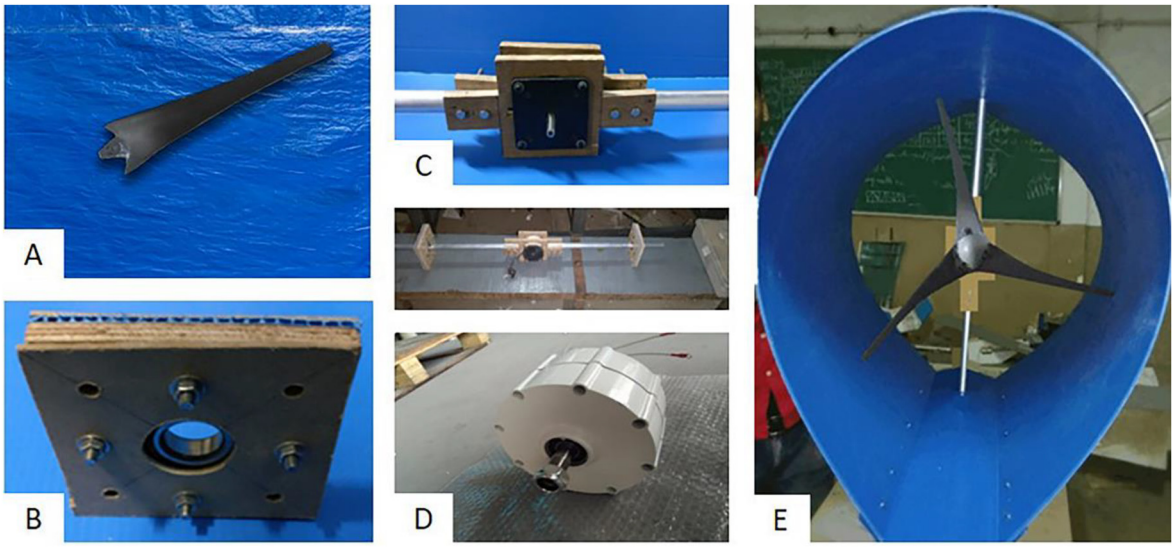

Figure 1: Airborne wind turbine part. (A) Blade, (B) Bearing fixture, (C) Motor fixture, (D) Motor, (E) Ducted turbine.

Figure 2: Airborne wind turbine experimental investigations.

In addition, reference (Tahir et al. 2017) contains detailed comparison research on the benefits and drawbacks of the PMG utilised in small wind turbines. Instead of using a wind turbine-specific controller, the power output is managed using a simple solar PV module maximum power point tracking (MPPT) controller. Even if an aerodynamically perfect rotor is developed, translating the improvements in aerodynamic efficiency into electrical power for the end-user requires a generator and controller system that is idealised. Small wind turbines lack the necessary spare parts, such as an ultrasonic anemometer or a lidar system, for accurate wind speed measurement. This condition leads to the increase in the production cost of the small turbine and further complicates the situation. MPPT control strategy for small wind turbines is presented in various studies, such as reference (Batt and Coates 2012).

Usually, small wind turbines produce modest voltages and much greater currents, which lead to increased I^2R losses. These losses might be eliminated by selecting an appropriate wire size, and consequently, in small wind turbines, trivial elements predominantly determine the performance of the turbine.

Airborne system design

Figure 3 shows the 3D CAD model of the airborne wind turbine system. The assembly was raised to the desired height using a helium-filled balloon. For the current performance evaluation purpose, the lifting capacity of the helium-filled balloon was estimated at 25 °C and one atmospheric pressure. Compared to air, which has a density of 1.1845 kg/m^3, helium has a density of 0.16394 kg/m^3. The buoyant force generated by the balloon is given in Eq. (6).

$$F_b = \rho_{air} * g * V \tag{6}$$

where g is the acceleration due to gravity, and V is the volume of air.

Where F_b is the upward thrust force created by the balloon, and conventionally for helium gas, this force must be greater than 1.5 times the combined weight due to the turbine, balloon skin, tethers, and all other devices, as shown in Eq. (7).

$$\begin{aligned} F_b &= \rho_{Air} \times g \times V_{balloon} \\ &= 1.5\,((M_{Helium} \times g) + (M_{Total} \times g)) \end{aligned} \tag{7}$$

As shown in Eq. (7), the mass of helium gas can be replaced by the density of the helium. Equation (8) shows the expression to determine the diameter of the balloon.

$$R = \sqrt[3]{(4.5 \times M_{Total})/4\pi(\rho_{Air} - 1.5\rho_{Helium})} \tag{8}$$

In Eq. (8), if the densities are substituted with their respective values, the equation reduces to $R = 0.73\sqrt[3]{M_{Total}}$.

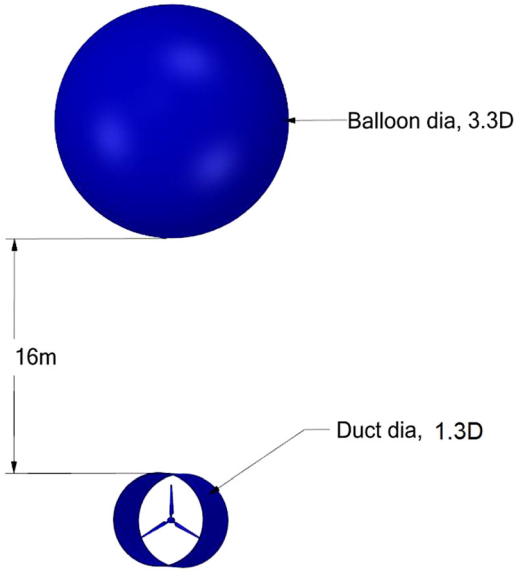

Figure 3: 3D CAD model of airborne wind turbine arrangements.

The device's overall weight was calculated to be 16 kg, which needed a balloon with a diameter of 12.25 ft., which matched the commercially available standard 12 ft. diameter balloon. As a result, the 12 ft. helium-filled balloon effortlessly raised the ducted wind turbine to the desired height.

Results and discussion

Wind turbines account for a sizable portion of the renewable energy spectrum. Airborne wind energy should be prioritised because it requires less capital investment than land-based large structures. The primary purpose of this experiment is to determine how much power the balloon-assisted micro-AWE system produces at various altitudes. The energy at various heights is estimated by raising the airborne system to predefined heights while simultaneously adjusting the tether wire lengths to position the system. The system must be allowed to reach a stable state by overcoming the ascending system's vibrations and oscillations.

Before making observations, it is necessary to check that the wind velocity has stabilised. The average value of the wind speed is considered most suited for avoiding inaccuracies due to the significant swings in wind speeds. It is vital to determine the wind speed in the area before installing a wind turbine.

The installation of a wind turbine, like the installation of a hydroelectric power station, necessitates extensive research to justify the site selection for wind turbine installation. Mountain ranges, woods, and high constructions all have an impact on wind velocity. The lowest layer of the wind is always turbulent due to the disturbances in its course. A wind layer that is impacted by terrain is known as an atmospheric boundary layer. The wind velocity varies with height, and at around 180 m, the wind velocity ceases to vary due to the absence of disturbances. As a result, 180 m is the minimum ideal height for harvesting wind energy from the air.

Air density is another essential component that influences power at higher altitudes. With each foot of height gained, the air density falls, resulting in less energy in the air.

As a result, wider diameter turbines are essential to capture energy in a less dense environment, adding to the system's cost. Hence, a careful balance is vital to create optimum energy at optimal heights.

Although different databases exist for assessing air velocity at various heights, Archer and Caldeira were the

first to capture the profile of wind power density at various heights in 2009 (Archer and Caldeira 2009).

Despite the fact that the study took place at altitudes ranging from 500 to 1200 m, wind densities vary greatly around the world due to a variety of causes. Figure 4 depicts the hourly wind speed distribution data for the Bangalore region over the course of a year at 10 and 80 m, respectively. Wind data for the Bengaluru region is acquired from the Government of Karnataka's meteorological department.

According to wind statistics, the available wind speed at the height of 250 m is approximately 6 m/s, which appears suitable for the microturbine. Getting higher altitude wind speed data is quite difficult than getting surface wind speed data.

The wind speed data can be modelled to the required accuracy using Eq. (9) for all practical purposes.

$$V_z = V_g (Z/Z_g)^{1/\alpha} \tag{9}$$

where,

V_z is the mean wind speed above ground level

V_g is the gradient wind speed assumed constant above the boundary layer

Z is the height above ground

Z_g is the nominal height of the boundary layer

α is the power-law coefficient

The power generated by the airborne turbine at different elevations was determined by an experimental investigation of the airborne wind turbine system. The balloon was filled with a predetermined quantity of commercially available helium gas to create enough lift force to raise the turbine assembly into the calculated height. The tether cables were connected to the electrical wires that carried electricity from the flying unit to the ground. Load estimations were performed on the ground using a 30 min timeframe for each reading. One of the critical observations made was the drifting of the wind turbine assembly due to the turbulence created by the balloon. The optimum distance between the balloon and the ducted wind turbine assembly was estimated through a CFD analysis, and the detailed study is submitted to another journal and is in the press for publication.

However, the airborne wind turbine assembly and the pressure probes arranged between the balloon and the turbine assembly in the CFD study are shown in Figure 5. The pressure difference at each level was estimated by varying the separation gap between the balloon and the turbine to 5, 10, and 15 m. Upon extensive CFD analysis of the pressure distribution in the gap, the 13 m separation gap is the optimal separation gap for the best performance, as shown in Figure 6.

In Figure 6, each line shows the pressure distribution from the balloon towards the turbine, and line 5 shows no pressure variation near the turbine. So, the gap between the balloon and the ducted wind turbine was maintained at 13 m for the experimental analysis.

The maximum height attainable by the airborne assembly is determined by the availability of the electrical wire, tether ropes, and the quality of balloon material. Because surrounding air pressure falls with increasing height, it is vital to check the balloon's resilience to prevent the balloon from bursting owing to a severe pressure

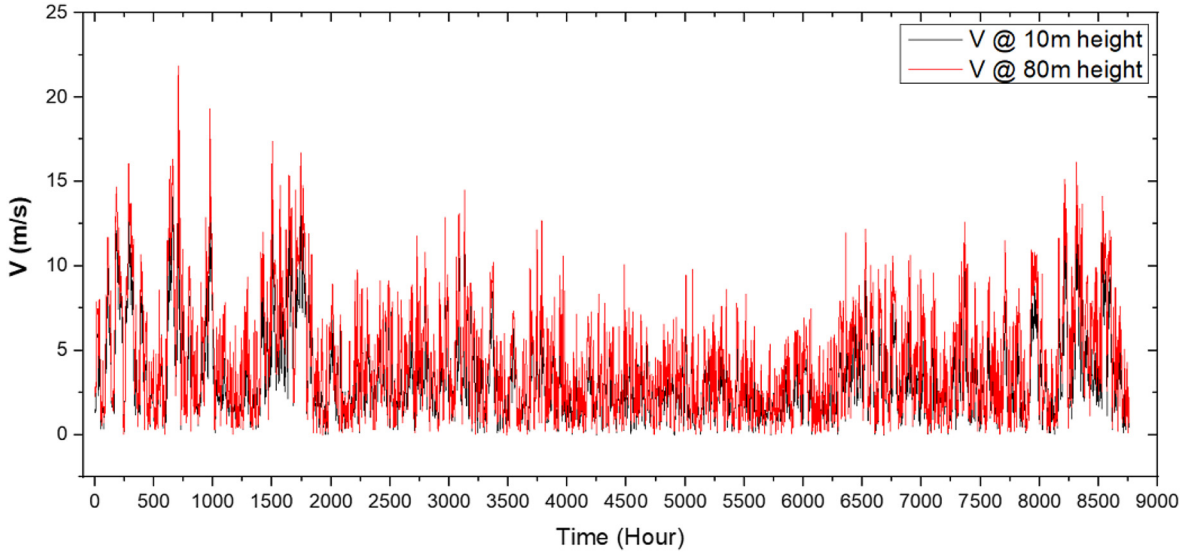

Figure 4: Wind speed distribution at 10 and 80 m heights (Weather History Download Bengaluru – Meteoblue).

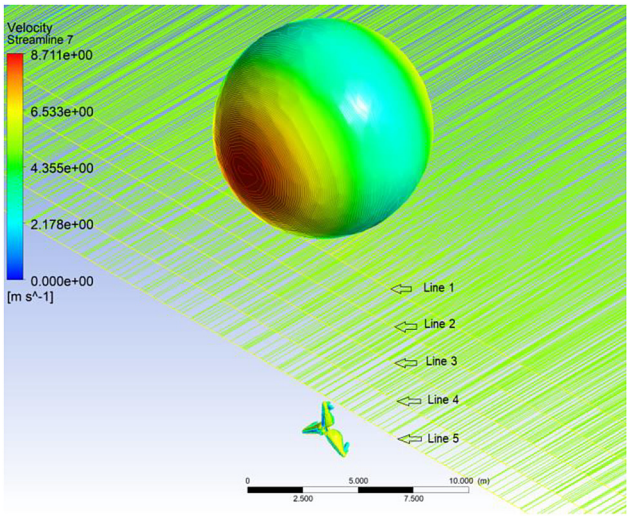

Figure 5: Pressure probes between the balloon and the turbine.

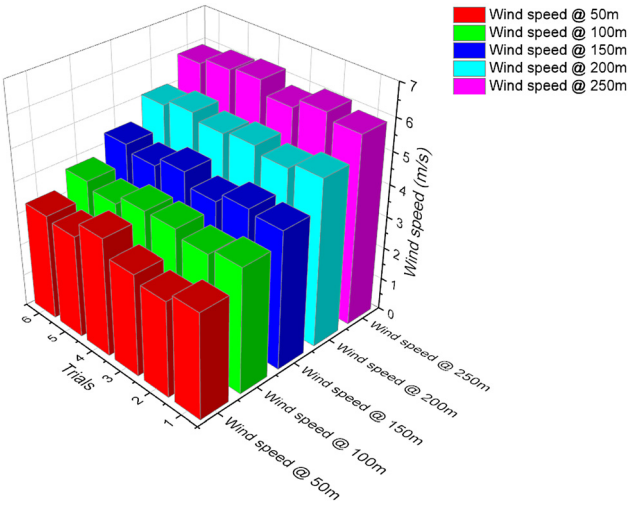

Figure 7: Wind speed distribution at different heights.

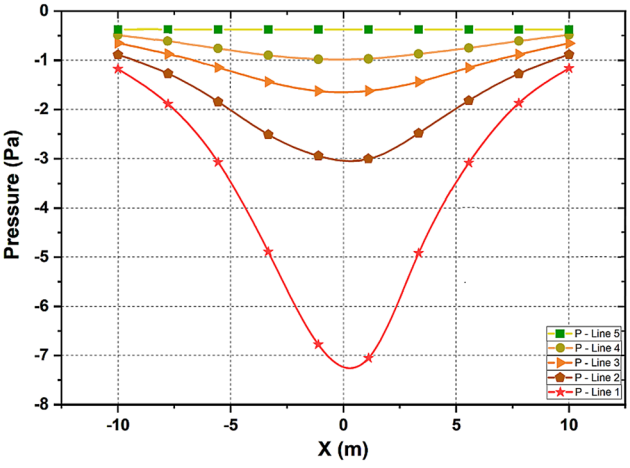

Figure 6: Pressure distribution between balloon and the turbine at 13 m gap.

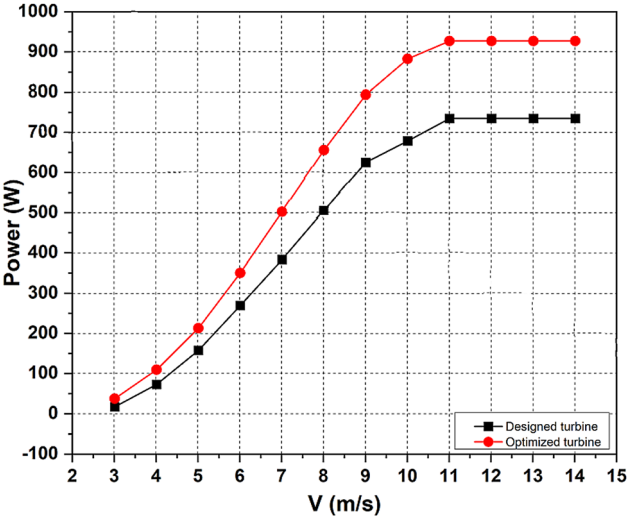

Figure 8: Theoretical power calculations for designed and optimized turbine.

disparity. Figure 7 illustrates the 3D plot of the wind speed data gathered with an anemometer at various heights and time intervals. Around 30 measurements were made to determine the wind speeds at various heights, with the maximum height set at 250 m. As can be seen in Figure 7, the wind speed increase with rising height.

Figure 8 illustrates the comparison of power produced by the initial design of the wind turbine and the optimised turbine. Before the actual working model of the wind turbine was produced, the design parameters were optimised, and the whole procedure is documented in reference (Noronha and Krishna 2020).

Every turbine is designed for a range of wind speeds, and as the wind speed surpasses, the wind turbine performance deteriorates. Figure 9 illustrates the dual plot of power produced by the turbine considering the maximum capacity and the power coefficient change with the wind speed. The turbine produces the highest power at a wind speed of 11 m/s, and the power curve lowers subsequently, demonstrating the decline in power production. Hence, for the present turbine, 11 m/s can be considered as the cut-off wind speed. In contrast, the power coefficient is observed hitting the maximum value for a wind speed of 5 m/s. However, the power coefficient and power curve intersection happen at 7.5 m/s where the power output is 400 W, and the power coefficient is 0.355, which is an ideal performance point for the present turbine.

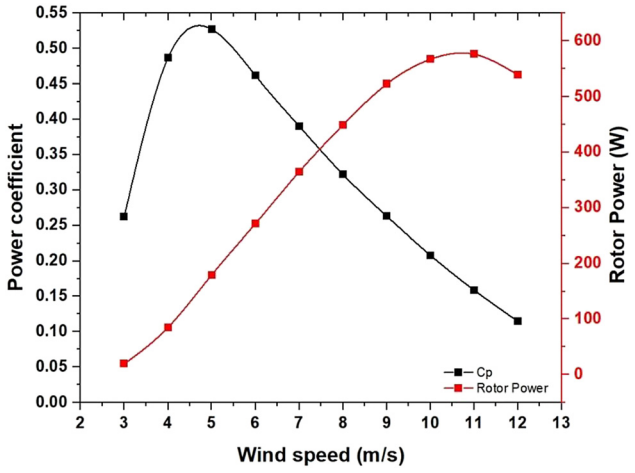

Figure 9: Power coefficient and rotor power produced at different wind speeds.

Figure 10 displays the scatter plot of the power generated by airborne wind turbine from 50 m height to 250 m height. The recorded data indicates an orderly distribution of values, with the average power values being precisely proportional to the wind speed. The cut-in speed of the turbine is estimated to be roughly 2.5 m/s based on the graph. The maximum air velocity reaches 7–7.5 m/s on rare occasions. However, the highest power is generated when the wind speed is between 3.5 and 5.5 m/s, which matches the area's actual wind speed range.

Though the ideal power generated by a wind turbine is proportional to the cube of wind velocity, Betz's limit restricts the actual power generated. The contrast between theoretical and real power created at each level is shown in Figure 11.

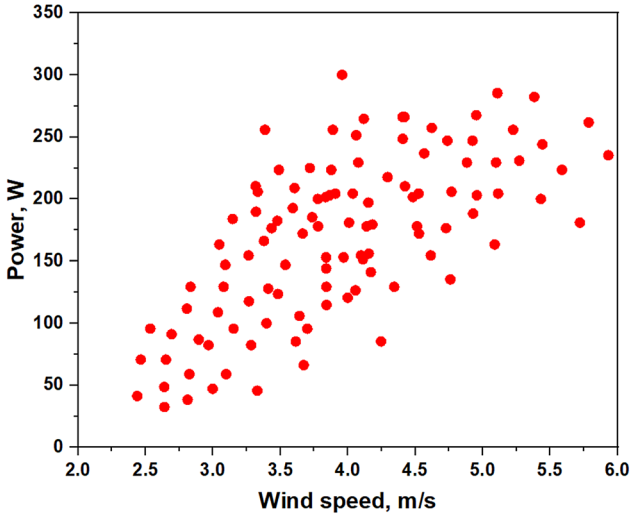

Figure 10: Experimental recordings of the turbine power from 50 to 250 m height.

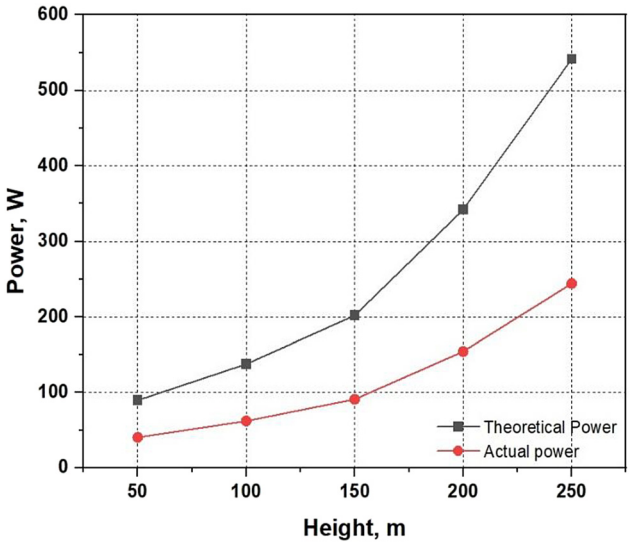

Figure 11: Theoretical and actual power produced.

The average power generated at each level is substantially less than the average theoretical power generated, and the gap between them rises with an increase in wind speed. The maximum power generated in the present study is 250 W at the height of 250 m, while the average wind speed is 6 m/s. The loss of power can be credited to numerous reasons such as the vibration of the airborne system, electrical and mechanical efficiency, turbulence in the wind, and other unexplained limits. The eventual success of an airborne wind turbine hinges on the ability of the device to produce enough energy for at least one family of five people. The annual energy output (AEP) of the system provides a decent picture of the viability of any energy system. The AEP of the present airborne wind

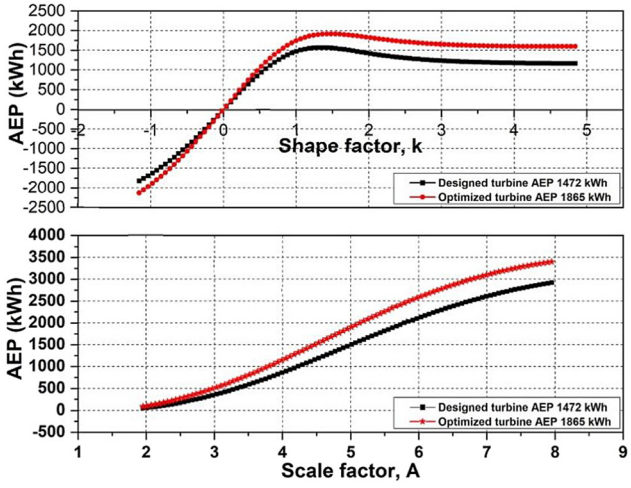

Figure 12: Annual energy production with shape factor and scale factor.

energy system, as shown in Figure 12, is around 1400 kWh which is quite impressive because per capita energy consumption in India is 1208 kWh as of 2020 (Govt. of India 2020). The preceding research shows that high-altitude wind power generation is viable in low wind speed situations.

Conclusions

Although the current study focuses on the experimental examination of AWES, the same approach might be improved to provide maximum power at a minimal cost. Future studies to understand the interplay between high-velocity winds and the AWES will rely heavily on numerical analysis of the AWES. In-depth research and indigenous technology can lower the cost of a single unit, making it more affordable to households, particularly in rural areas. The authors want to continue their research by designing appropriate ducts that will improve the performance of the airborne wind turbine. Even though the scientific community is aware of airborne wind energy systems, no research focusing on their potential has yet begun. The viability of harnessing wind energy in low-wind areas like Bangalore, India, is examined in this study, although the same technology can be successfully deployed in any part of the world without modification. Because airborne wind energy is universal, there are several experimental and numerical research opportunities in this field.

Author contributions: All the authors have accepted responsibility for the entire content of this submitted manuscript and approved submission.
Research funding: None declared.
Conflict of interest statement: The authors declare no conflicts of interest regarding this article.

References

Archer, C. L., and K. Caldeira. 2009. "Global Assessment of High-Altitude Wind Power." *Energies* 2 (2): 307–19.

Argatov, I., P. Rautakorpi, and R. Silvennoinen. 2009. "Estimation of the Mechanical Energy Output of the Kite Wind Generator." *Renewable Energy* 34 (6): 1525–32.

Baheri, A., and C. Vermillion. 2017. "Altitude Optimization of Airborne Wind Energy Systems: A Bayesian Optimization Approach." *2017 American Control Conference (ACC)* 1365–70, https://doi.org/10.23919/ACC.2017.7963143.

Batt, N., and C. Coates. 2012. "Maximising Output Power of Self-Excited Induction Generators for Small Wind Turbines." In *Proceedings – 2012 20th International Conference on Electrical Machines*, ICEM: Marseille, France 2012, 2105–11.

Bergey, K. H. 1979. "The Lanchester-Betz Limit (Energy Conversion Efficiency Factor for Windmills)." *Journal of Energy* 3 (6): 382–90.

Boyerahmadi, S., N. Amjady, and A. Rezaey. 2012. "A New Approach for Classification of Airborne Wind Energy Generation Systems." *Journal of Basic and Applied Scientific Research* 2 (10): 10752–7.

Dighe, V. V., G. de Oliveira, F. Avallone, and G. J. W. van Bussel. 2019. "Characterization of Aerodynamic Performance of Ducted Wind Turbines: A Numerical Study." *Wind Energy* 22 (12): 1655–66.

Dighe, V. V., F. Avallone, O. Igra, and G. van Bussel. 2019. "Multi-Element Ducts for Ducted Wind Turbines: A Numerical Study." *Wind Energy Science* 4 (3): 439–49.

Fagiano, L., M. Milanese, and D. Piga. 2010. "Optimization of High-Altitude Wind Energy Generators." *Airborne Wind Energy Conference 2010* 22: 2055–83.

Govt. of India. 2020. *Growth of Electricity Sector in India from 1947–2020*. New Delhi, India: Ministry of New and Renewable Energy. https://cea.nic.in/wp-content/uploads/pdm/2020/12/growth_2020.pdf (accessed July 19, 2021).

Hwang, I. S., W. Kang, and S. J. Kim. 2011. "An Airborne Cycloidal Wind Turbine Mounted Using a Tethered Balloon." *International Journal of Aeronautical and Space Sciences* 12 (4): 354–9.

Kesby, J., D. Bradney, and P. D. Clausen. 2017. "Determining the Performance of a Diffuser Augmented Wind Turbine Using a Combined CFD/BEM Method." *Renewable Energy and Environmental Sustainability* 2: 22.

Khalil, A., K. Alfaitori, and A. Asheibi. 2016. "Modeling and Control of PV/Wind Microgrid." In *2016 7th International Renewable Energy Congress (IREC)*, 2016, IEEE: Hammamet, Tunisia, pp. 1–6, https://doi.org/10.1109/IREC.2016.7478916.

Manalis, M. S. 1976. "Airborne Windmills and Communication Aerostats." *Journal of Aircraft* 13 (7): 543–4.

Manwell, J. F., J. G. McGowan, and A. L. Rogers. 2010. *Wind Energy Explained: Theory, Design and Application*. UK: John Wiley & Sons Ltd.

Noronha, N. P., and M. Krishna. 2020. "Design and Analysis of Micro Horizontal Axis Wind Turbine Using MATLAB and QBlade." *International Journal of Advanced Science and Technology* 29 (10S): 8877–85.

Rajab, Z., Y. Sassi, A. Taher, A. Khalil, and F. Mohamed. 2019. "A Practical Seasonal Performance Evaluation of Small Wind Turbine in Urban Environment." *Wind Engineering* 43 (4): 344–58.

Tahir, A., Z. Rajab, A. Hammoda, S. Greibea, L. Alakeili, D. Elshaibani, and F. Mohamed. 2017. "Genetic Algorithm–Based Calculation of the Excitation Capacitance of a Self-Excited Induction Generator for Stable Voltage Operation over Load and Speed Variations." *Wind Engineering* 41 (6): 421–30.

Weather History Download Bengaluru – Meteoblue. https://www.meteoblue.com/en/weather/archive/export/bengaluru_india_1277333 (accessed July 17, 2021).

Wood, D. 2010. "Small Wind Turbines for Remote Power and Distributed Generation." *Wind Engineering* 34 (3): 241–54.

Zafar, S., M. Gadalla, and M. I. Al-Naiser. 2016. "Performance Evaluation of a Novel Small Wind Turbine: UAE Case Study." In *American Society of Mechanical Engineers, Power Division (Publication) POWER*, 2016-January. Charlotte, North Carolina, USA: American Society of Mechanical Engineers, Power Division (Publication) POWER.

Zanon, M., S. Gros, J. Andersson, and M. Diehl. 2013. "Airborne Wind Energy Based on Dual Airfoils." *IEEE Transactions on Control Systems Technology* 21 (4): 1215–22.